



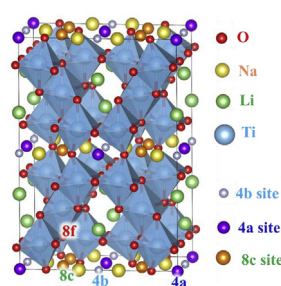
Review article

Recent advances in the research of $\text{MLi}_2\text{Ti}_6\text{O}_{14}$ ($\text{M} = 2\text{Na}, \text{Sr}, \text{Ba}, \text{Pb}$) anode materials for Li-ion batteriesTing-Feng Yi^{a,b,*}, Yan-Rong Zhu^a, Wei Tao^a, Shaohua Luo^{a,b,**}, Ying Xie^{c,***}, Xi-Fei Li^d^a School of Resources and Materials, Northeastern University at Qinhuangdao, Qinhuangdao 066004, PR China^b School of Materials Science and Engineering, Northeastern University, Shenyang 110819, PR China^c Key Laboratory of Functional Inorganic Material Chemistry, Ministry of Education, School of Chemistry and Materials Science, Heilongjiang University, Harbin 150080, PR China^d Institute of Advanced Electrochemical Energy, Xi'an University of Technology, Xi'an 710048, PR China

HIGHLIGHTS

- Progress of $\text{MLi}_2\text{Ti}_6\text{O}_{14}$ is summarized in details for the first time.
- An understanding on modifying $\text{MLi}_2\text{Ti}_6\text{O}_{14}$ from various aspects is summarized.
- Key strategies for improving the cycling stability of $\text{MLi}_2\text{Ti}_6\text{O}_{14}$ is discussed.
- Strategies in the development of $\text{MLi}_2\text{Ti}_6\text{O}_{14}$ -based batteries are discussed.

GRAPHICAL ABSTRACT



ARTICLE INFO

Keywords:

Lithium-ion battery
Titanate
Anode material
Cycling stability
In situ X-ray diffraction

ABSTRACT

Lithium-ion batteries (LIBs) are considered as a promising power source for electric vehicles and electronic products such as mobile phones, laptops, and tablets. The anode material plays a crucial role in the reliability and safety of LIBs. Among the anode candidates, $\text{MLi}_2\text{Ti}_6\text{O}_{14}$ ($\text{M} = 2\text{Na}, \text{Sr}, \text{Ba}, \text{Pb}$) materials have very good prospects due to their excellent safety, good structure stability, negligible volume change, and suitable voltage plateau of about 1.3–1.4 V (vs. Li^0/Li^+). However, $\text{MLi}_2\text{Ti}_6\text{O}_{14}$ materials frequently sustain serious capacity decay at high rate due to the poor electronic and ionic conductivities. Therefore, it is very meaningful to summarize comprehensively and scientifically the advances of this material family from all aspects. The main objective of the review is aimed to summarize various proposed strategies (i.e. material treatment, morphology control, surface modification, and cation doping) and the breakthroughs to enhance the rate capacity and cycling stability of the $\text{MLi}_2\text{Ti}_6\text{O}_{14}$ materials. The review will provide some insights into the structures and performance issues, which will be helpful for the design and optimization of the $\text{MLi}_2\text{Ti}_6\text{O}_{14}$ materials.

1. Introduction

With the rapid development of the economy, the consumption of

traditional energy sources such as fossil fuel, coal, and natural gas causes more and more problems. Although solar energy and other renewable energies have attracted a lot of attention, most of them have

* Corresponding author. School of Resources and Materials, Northeastern University at Qinhuangdao, Qinhuangdao 066004, PR China.

** Corresponding author. School of Resources and Materials, Northeastern University at Qinhuangdao, Qinhuangdao 066004, PR China.

*** Corresponding author.

E-mail addresses: tfyhit@163.com (T.-F. Yi), tianyanglsh@163.com (S. Luo), xieying@hlju.edu.cn (Y. Xie).

not been widely used due to many reasons. At the same time, many researchers have also devoted themselves to other energy storage and conversion techniques. Among them, LIBs have gained great success [1,2] and become indispensable in our daily life because of their high energy density, excellent cycling stability, and safety. As we know, LIBs have been used in business application for energy supplies of EVs (electric vehicles) and electronic products, such as mobile phones, laptops, and tablets [3]. At present, the commercial cathode are mainly composed of LiFePO_4 [4–7], LiCoO_2 [8,9] or LiMn_2O_4 [10–12], while the commercial anode materials are mainly graphite-based materials [13–19]. As well-known, graphite-based materials are low cost with a good stability and processability, and they also possess high electronic conductivity and low voltage plateau [13]. Lithium ions can be intercalated and de-intercalated into/from graphite-based anode during charging/discharging processes in a narrow voltage window between 0.05 and 0.3 V (vs. Li/Li^+) through multistage phase transitions [14]. It was reported that the voltage of the final phase transition from LiC_{12} to LiC_6 is as low as 0.065 V (vs. Li/Li^+), indicating the maximum overpotential during charge does not exceed 0.065 V [15]. Hence, one safety issue appears, and it is related to the dendritic lithium growth on the anode surface at high charging current, because graphite materials will approach nearly 0 V (vs. Li/Li^+) at the end of Li insertion [16]. In addition, the formation of the amorphous solid electrolyte interphase (SEI) film on graphite anode during cycling will generate a matrix expansion and lead to a longer diffusion path for Li ions, resulting in a poor cycling stability and a low reversible capacity at high current density [17,18]. Moreover, it was found that the stability of graphite-based anode is also highly dependent on the composition of the electrolyte lithium salt and solution [19]. Therefore, searching for new and highly safe anode materials becomes one of the most important research directions in the LIB industries.

Among all the anode materials, titanate-based materials have received significant attention due to their unique performance and structural advantages [20–26]. $\text{Li}_4\text{Ti}_5\text{O}_{12}$ is considered as a promising alternative to commercial graphite because of its high structural stability, high potential plateau (1.5 V vs. Li^0/Li^+), and excellent cycle property [27–31]. The relatively high potential plateau avoids the formation of lithium dendrites, yet it also reduces the energy density of the full battery. To improve the energy and power densities within the stable region of the electrolyte, some novel titanate-based materials with a lower potential plateau are expected. The mixed alkali titanium oxides ($\text{MLi}_2\text{Ti}_6\text{O}_{14}$) have been proposed and regarded as perfect candidates to replace $\text{Li}_4\text{Ti}_5\text{O}_{12}$ for future applications [32–36]. $\text{MLi}_2\text{Ti}_6\text{O}_{14}$ ($M = \text{Na}$ [37–45], Sr [46–55], Ba [35,52–55], Pb [52]) can be considered as $\text{Li}_2\text{O}-\text{MO}-\text{TiO}_2$ ternary oxide systems. The introduction of alkali derivatives into titanium oxides will reduce the working voltage of $\text{MLi}_2\text{Ti}_6\text{O}_{14}$ [55–57], which in turn increases the mass and volume energy densities of the full battery. A low voltage of anode means that the full battery has a high open circuit voltage, and then contributes to increase of mass energy density and volume energy density of the full battery. The different behavior can be attributed to the special three-dimensional framework of $\text{MLi}_2\text{Ti}_6\text{O}_{14}$ ($M = 2\text{Na}, \text{Sr}, \text{Ba}, \text{Pb}$). The twisted titanium oxide octahedrons in $\text{MLi}_2\text{Ti}_6\text{O}_{14}$ is connected through a common edge and two vertex, forming a crystalline skeleton, and a channel is formed along b axis. The independent and deformed lithium-oxygen tetrahedrons are embedded within the TiO_6 network. Such a structure facilitates the intercalation and deintercalation of lithium ions. Except of the open circuit voltage (OCV) consideration, $\text{MLi}_2\text{Ti}_6\text{O}_{14}$ also exhibits different characteristics. $\text{BaLi}_2\text{Ti}_6\text{O}_{14}$ and $\text{PbLi}_2\text{Ti}_6\text{O}_{14}$ show a lower reversible capacity than $\text{Na}_2\text{Li}_2\text{Ti}_6\text{O}_{14}$ and $\text{SrLi}_2\text{Ti}_6\text{O}_{14}$, even at low current density, while the element abundance of Na (2.83%) with respect to that of Sr (0.04%) will significantly reduce the cost of $\text{Na}_2\text{Li}_2\text{Ti}_6\text{O}_{14}$. In addition, $\text{Na}_2\text{Li}_2\text{Ti}_6\text{O}_{14}$ shows a lower potential plateau (1.25 V vs. Li/Li^+) than other $\text{MLi}_2\text{Ti}_6\text{O}_{14}$ compounds, and its working potential is also superior to the novel $\text{Li}_2\text{MTi}_3\text{O}_8$ ($M = \text{Zn}, \text{Co}, \text{Cu}, \text{Mn}$) [58–61].

Table 1Lattice parameters of the $\text{MLi}_2\text{Ti}_6\text{O}_{14}$ ($M = 2\text{Na}, \text{Sr}, \text{Ba}, \text{Pb}$).

Crystal	a	b	c
$\text{Na}_2\text{Li}_2\text{Ti}_6\text{O}_{14}$	16.484 Å	5.737 Å	11.220 Å
$\text{SrLi}_2\text{Ti}_6\text{O}_{14}$	16.566 Å	11.148 Å	11.468 Å
$\text{BaLi}_2\text{Ti}_6\text{O}_{14}$	16.575 Å	11.268 Å	11.579 Å
$\text{PbLi}_2\text{Ti}_6\text{O}_{14}$	16.649 Å	11.146 Å	11.494 Å

In consideration of the safety, cost, and working potential, $\text{Na}_2\text{Li}_2\text{Ti}_6\text{O}_{14}$ anode becomes a promising candidate for the fabrication of full batteries. For example, a full battery constructed by LiFePO_4 cathode and $\text{Na}_2\text{Li}_2\text{Ti}_6\text{O}_{14}$ anode will deliver a OCV of about 2.1 V [62], while the values for $\text{Na}_2\text{Li}_2\text{Ti}_6\text{O}_{14}/\text{LiCoO}_2$ [63], $\text{Na}_2\text{Li}_2\text{Ti}_6\text{O}_{14}/\text{LiCo}_{1/3}\text{Mn}_{1/3}\text{Ni}_{1/3}\text{O}_2$ [64], $\text{Na}_2\text{Li}_2\text{Ti}_6\text{O}_{14}/\text{LiMnPO}_4$ [65], $\text{Na}_2\text{Li}_2\text{Ti}_6\text{O}_{14}/\text{LiMn}_2\text{O}_4$ [66], and $\text{Na}_2\text{Li}_2\text{Ti}_6\text{O}_{14}/\text{LiNi}_{0.5}\text{Mn}_{1.5}\text{O}_4$ [67] are 2.6, 2.6, 2.7, 2.8, and 3.4 V, respectively. Unfortunately, like $\text{Li}_4\text{Ti}_5\text{O}_{12}$, the poor lithium diffusion coefficient (10^{-17} – $10^{-15} \text{ cm}^2 \text{ s}^{-1}$) and the poor electrical conductivity (10^{-16} – $10^{-14} \text{ S cm}^{-1}$) of $\text{MLi}_2\text{Ti}_6\text{O}_{14}$ have limited their full capability at high current density application. To overcome the problems and improved the electrochemical performance of $\text{Li}_2\text{MTi}_3\text{O}_8$, structural modulation and optimization on this family are thus very necessary. Therefore, the main objective of this review is aimed to emphasize various proposed strategies and breakthroughs to enhance the rate capacity and cycling stability of the $\text{MLi}_2\text{Ti}_6\text{O}_{14}$ materials, which will be beneficial for their designs in the near future.

2. Structure of $\text{MLi}_2\text{Ti}_6\text{O}_{14}$ ($M = 2\text{Na}, \text{Sr}, \text{Ba}, \text{Pb}$)

The lattice parameters of $\text{MLi}_2\text{Ti}_6\text{O}_{14}$ ($M = 2\text{Na}, \text{Sr}, \text{Ba}, \text{Pb}$) listed in Table 1 can be obtained from a single-crystal structure refinement. All the lattice parameters for $\text{MLi}_2\text{Ti}_6\text{O}_{14}$ ($M = \text{Sr}, \text{Ba}, \text{Pb}$) are similar. The slight difference of the parameters was due to the ionic radius differences of Sr^{2+} , Ba^{2+} and Pb^{2+} ions. Such parameters are in good accordance with the reported values by Koseva [54] et al. $\text{MLi}_2\text{Ti}_6\text{O}_{14}$ ($M = \text{Sr}, \text{Ba}, \text{Pb}$) structures are made up of a three-dimensional $[\text{TiO}_6]$ octahedron network through sharing corners and edges, and the 11-fold-coordinated polyhedrons are formed between alkali-earth ions and oxygen [53]. $[\text{LiO}_4]$ tetrahedrons are located within the void space of the $[\text{TiO}_6]$ tunnels. It was reported that the space groups for $\text{SrLi}_2\text{Ti}_6\text{O}_{14}$, $\text{BaLi}_2\text{Ti}_6\text{O}_{14}$, and $\text{PbLi}_2\text{Ti}_6\text{O}_{14}$ are all $Cmca$. But for $\text{Na}_2\text{Li}_2\text{Ti}_6\text{O}_{14}$, because two Na ions are equivalent to one bivalent metal ion, the 11-fold-coordinated positions were all filled. $\text{Na}_2\text{Li}_2\text{Ti}_6\text{O}_{14}$ thus possesses a higher symmetry, which belongs to the $Fmmm$ space group. The crystal structures of $\text{Na}_2\text{Li}_2\text{Ti}_6\text{O}_{14}$ and $\text{PbLi}_2\text{Ti}_6\text{O}_{14}$ are given in Fig. 1, and the positions were labeled according to the Wyckoff tables listed in the Table S1 and Table S2 of the Supplemental Information (SI). The representation (4a) was constructed by a multiplicity (4) and a Wyckoff letter (a). The former was related to the symmetry of the crystal, while the latter always began with letter a and increased in the order of alphabet.

The detailed crystal structure of $\text{Na}_2\text{Li}_2\text{Ti}_6\text{O}_{14}$ is showed in Fig. 1 (a, b). It can be found that TiO_6 octahedrons are connected via shared oxygen along three directions, and several possible tunnels for lithium diffusions are thus formed, as characterized by the green rectangle in Fig. 1 (a, b). Furthermore, sodium species are distributed within two non-equivalent (100) crystal planes with x coordinates of 0.0 or 0.5, respectively. The special arrangement of sodium leads to the formation of a C_2 axis along $[100]$ direction and the formation of a symmetric plane perpendicular to the two-fold axis. Therefore, the symmetry of $\text{Na}_2\text{Li}_2\text{Ti}_6\text{O}_{14}$ crystal along x axis can be denoted as $2/m$. Similarly, the other two directions also possess $2/m$ symmetries, and the space group for $\text{Na}_2\text{Li}_2\text{Ti}_6\text{O}_{14}$ crystal is finally determined to be $Fmmm$.

According to the Wyckoff representation, it can be identified that 4a, 4b, and 8c sites in $\text{Na}_2\text{Li}_2\text{Ti}_6\text{O}_{14}$ crystal are all empty, and they are

Download English Version:

<https://daneshyari.com/en/article/7724631>

Download Persian Version:

<https://daneshyari.com/article/7724631>

[Daneshyari.com](https://daneshyari.com)